Coulomb drag in coupled 2D-2D and 2D-1D cylindrical quantum wells

1995 J. Phys.: Condens. Matter 7 9785

(http://iopscience.iop.org/0953-8984/7/50/013)

J. Phys.: Condens. Matter 7 (1995) 9785–9798. Printed in the UK

Coulomb drag in coupled 2D–2D and 2D–1D cylindrical quantum wells

G Qin†‡

† CCAST (World Laboratory), PO Box 8730, Beijing 100080, People's Republic of China
‡ Department of Physics, Nanjing University, Nanjing 210008, People's Republic of China§

Received 12 June 1995, in final form 26 September 1995

Abstract. To study the Coulomb drag resistivity of barrier-coupled 2D−1D and 2D−2D systems as well as the transition behaviour between them, we suggest investigation of a system which is composed of a couple of barrier-separated cylindrical δ quantum wells (CDWs) with a common cylindrical symmetry axis. We find that for coupled 2D−1D CDWs, the momentum relaxation rate, τ_D^{-1}, is approximately proportional to T^4, while for coupled 2D−2D CDWs, it is proportional to T^2 which is in accord with the characteristic behaviour of the momentum relaxation rate in coupled 2D−2D planes. In the transition region from coupled 2D−1D to 2D−2D CDWs, τ_D^{-1} is proportional to T^n with n reduced from 4 to 2 gradually. In addition, quite unlike the approximate $d^{-2.4}$-dependence of momentum relaxation rate divided by T_{max}^2 in coupled 2D−2D planes, due to the quantization of the circular motion round a cylindrical symmetry axis, for coupled 2D−1D CDWs the momentum relaxation rate divided by T_{max}^4 is approximately proportional to d^{-3} times a nearly periodic function of d, while for coupled 2D−2D CDWs, the momentum relaxation rate divide by T_{max}^2 is approximately proportional to $d^{-2.4}$ times a nearly periodic function of d, where d is the distance between two CDWs.

1. Introduction

The characteristic energy dependence of the electron–electron scattering rate is due to the phase-space restrictions that apply to the mutual scattering of particles in a nearly degenerate gas. These restrictions are different for systems with different dimensionalities. In a three-dimensional electron gas at zero temperature, the electron–electron scattering rate $1/\tau(\epsilon)$ depends on the electron energy ϵ according to $1/\tau(\epsilon) \propto (\epsilon - \mu)^2$, where μ is the chemical potential. At finite temperatures this characteristic energy dependence yields relaxation rates that are proportional to T^2. For a two-dimensional electron gas this scattering rate at zero temperature is proportional to $(\epsilon-\mu)^2\ln|\epsilon-\mu|$ [1]. At finite temperatures the corresponding relaxation rates become proportional to T^2 ln T. In the past few years, the Coulomb drag problem in barrier-coupled systems has attracted considerable research interest because it provides a way of probing electron–electron interactions between two systems which play a crucial role both in basic theoretical research and experimental studies. The research results in this field show also that the relaxation rates between two barrier-separated systems depend sensitively on the dimensionality of the two systems coupled to each other. The effect has been considered in coupled 3D−3D, 3D−2D, 2D−2D and 1D−1D systems by a number of different authors [2–5], but none of them have ever discussed the mutual drag between the 2D system and the 1D system as well as the transition behaviour of the Coulomb drag

§ Mailing address.

0953-8984/95/509785+14$19.50

from coupled 2D–2D to coupled 2D–1D and from coupled 2D–1D to coupled 1D–1D systems.

In a cylindrical quantum well (CQW) [6, 7], the electrons are confined in the cylindrical potential well with inside radius a_1 and outside radius a_2, and are free to move in the well. If a_1 tends to a_2, i.e., the electron density profile in the radial direction is a δ-function, the electron gas is confined in a cylindrical surface, and a CQW is reduced to a CDW as we call it from now on. In this paper we consider a barrier-coupled CDW system as shown schematically in figure 1 which is composed of two CDWs with a common cylindrical symmetry axis (i.e., the two CDWs are coaxial), of radii a and b respectively ($b > a$ and $b - a = d$). Their length, L, tends to infinity. Such a coupled CDW model would be an interesting system to study because we know well that when we reduce the radius of a CDW, the dimensionality of its electron gas changes from 2D to 1D at a critical radius r_c which is determined by the electron area density [6–8]. Therefore when we change the radii of both CDWs of a coupled CDW system, we can study the Coulomb drag properties between 2D and 2D, 2D and 1D or 1D and 1D electron gases, and study the transition behaviour between them.

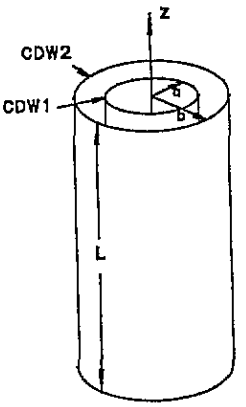

Figure 1. A schematic drawing of the barrier-coupled CDW system.

2. Drag resistivity in coupled CDWs

After a current I_2 along the direction of cylindrical symmetry axis (the z-direction) is driven in the outer CDW with radius b, one measures the voltage difference V_1 which is induced in the inner CDW with radius a under the condition that no current flows in this CDW. The current per unit width is $j_2 = I_2/(2\pi b)$, while the magnitude of the electric field strength, which prevents the electrons in the inner CDW from being dragged along by the current in the outer CDW, is $E_1 = V_1/l$, where l denotes the distance between the probes used to measure the voltage difference. The drag resistivity is defined by

$$\rho_D = \frac{E_1}{j_2} = \frac{2\pi b V_1}{I_2 l}. \tag{1}$$

Experimentally, E_1 is found to be proportional to drift velocity u_2 which is defined as

$$j_2 = n_2 e u_2 \tag{2}$$

where n_2 is the number of electrons per unit area in the outer CDW, while e is the elementary charge. The coefficient relating E_1 and u_2 is the drag mobility μ_D which is defined by

$$\mu_D = \frac{u_2}{E_1}. \tag{3}$$

The mobility μ_D may in turn be expressed in terms of the momentum relaxation rate $1/\tau_D$ according to

$$\mu_D = \frac{e}{\mu^*}\tau_D. \tag{4}$$

As a result, the drag resistivity, which has the dimension of a resistance, may also be written as

$$\rho_D = \frac{\mu^*}{n_2 e^2 \tau_D} \tag{5}$$

where μ^* is the effective mass of conduction electrons. The theoretical calculation is aimed at expressing the drag resistivity ρ_D or the momentum relaxation rate $1/\tau_D$ as a function of temperature T and the distance d separating the two CDWs.

3. The momentum relaxation rate

The noninteracting single-particle ground-state energy and wave function for the electron with effective mass μ^* in the CDW with radius r_0 can be written as

$$|\nu\rangle = |0, m, k\rangle = \exp(ikz + im\phi)\xi_0(r) \tag{6}$$

with $|\xi_0(r)|^2 = \delta(r - r_0)/r$ and

$$\epsilon_\nu = \varepsilon_0 + \frac{\hbar^2}{2\mu^*}(k^2 + m^2/r_0^2). \tag{7}$$

The momentum relaxation rate is determined by using the linearized Boltzmann equation [5]. The linearized collision integral in cylindrical coordinates is

$$\left(\frac{\partial f_1}{\partial t}\right)_{coll} = -\frac{1}{(2\pi)^2 ab}\sum_{\sigma_2,\sigma_{1'},\sigma_{2'}}\sum_{m_2,m_{1'}}\int\frac{dk_2}{(2\pi)}\int\frac{dk_{1'}}{(2\pi)}w(1,2;1',2')(\psi_2 - \psi_{2'})$$
$$\times f_1^0 f_2^0(1 - f_{1'}^0)(1 - f_{2'}^0)\,\delta(\epsilon_1 + \epsilon_2 - \epsilon_{1'} - \epsilon_{2'}) \tag{8}$$

where f^0 is the equilibrium distribution function. For brevity, the quantum number sets $(0, m_1, k_1)$, $(0, m_2, k_2)$ etc are labelled as 1, 2, ..., and the quantities referring to the inner CDW (CDW 1) are labelled $1, 1'$, and, similarly, those referring to the outer CDW (CDW 2) are labelled $2, 2'$. $w(1, 2; 1', 2')$ determines the probability that two electrons in states 1 and 2 will scatter to $1'$ and $2'$. Also, we have $m_{2'} = m_1 + m_2 - m_{1'}$ and $k_{2'} = k_1 + k_2 - k_{1'}$ because of conservation of angular momentum and momentum. In terms of the momentum conservation, the difference between two deviation functions can be written as

$$\psi_2 - \psi_{2'} = -\frac{\hbar e \tau_2 E_2}{\mu^* k_B T}(k_{1'} - k_1) \tag{9}$$

where E_2 is the electric field in CDW 2, directed along the z-axis, and τ_2 is an energy-independent momentum relaxation time. We now multiply both sides of equation (8) by k_1 and sum over the state (m_1, k_1, σ_1). The term $k_1(k_{1'} - k_1)$ in the integrand can be replaced by $-(k_{1'} - k_1)^2/2$ due to the symmetry of the remaining part of the integrand with respect

to the interchange of 1 and 1′. After completing the integration by parts on the left-hand side of the equation, we get

$$\frac{eE_1n_1}{\hbar}=\left(-\frac{\hbar e\tau_2E_2}{2(2\pi)^3a^2b\mu^*k_BT}\right)\sum_{\sigma_1,\sigma_2,\sigma_{1'},\sigma_{2'}}\sum_{m_{1'},m_1,m_2}\int\frac{\mathrm{d}k_{1'}}{2\pi}\int\frac{\mathrm{d}k_1}{2\pi}\int\frac{\mathrm{d}k_2}{2\pi}w(1,2;1'2')q^2$$
$$\times f^0_1f^0_2(1-f^0_{1'})(1-f^0_{2'})\,\delta(\epsilon_1+\epsilon_2-\epsilon_{1'}-\epsilon_{2'}) \tag{10}$$

where q is the wave-vector transfer given by $q=k_{1'}-k_1$.

By using the Born approximation, we get

$$\sum_{\sigma_1\sigma_2\sigma_{1'}\sigma_{2'}}w(1,2;1',2')=\frac{2\pi}{\hbar}4|e\phi_{\Delta m}(q)|^2 \tag{11}$$

where $e\phi_{\Delta m}(q)$ is the Fourier transform of the effective interaction. The expression for the coupled CDW system will be given in the next section.

The intrasubband quasi-two-dimensional polarizability is defined by [6]

$$\chi_{0,0;r_0}(q,\Delta m,\omega)=-\left(\frac{1}{S}\right)\sum_{m_1,k_1,\sigma_1}\frac{f_0(\epsilon_1)-f_0(\epsilon_{1'})}{\epsilon_1-\epsilon_{1'}+\hbar\omega+\mathrm{i}\delta} \tag{12}$$

where S is the surface area of the CDW, $\Delta m=m_{1'}-m_1$ and $q=k_{1'}-k_1$. So

$$\mathrm{Im}\ \chi_{0,0;r_0}(q,\Delta m,\omega)=\left(\frac{1}{S}\right)\sum_{m_1,k_1,\sigma_1}(f_0(\epsilon_1)-f_0(\epsilon_{1'}))\pi\,\delta(\epsilon_1-\epsilon_{1'}+\hbar\omega). \tag{13}$$

By using

$$\delta(\epsilon_1+\epsilon_2-\epsilon_{1'}-\epsilon_{2'})=\hbar\int_{-\infty}^{+\infty}\mathrm{d}\omega\,\delta(\epsilon_1-\epsilon_{1'}+\hbar\omega)\,\delta(\epsilon_2-\epsilon_{2'}-\hbar\omega) \tag{14}$$

and

$$f_0(\epsilon)[1-f_0(\epsilon+\hbar\omega)]=[f_0(\epsilon)-f_0(\epsilon+\hbar\omega)]/[1-\exp(-\hbar\omega/k_BT)] \tag{15}$$

together with equations (3), (4), (13) and $u_2=e\tau_2E_2/\mu^*$, we may transform equation (10) into

$$\frac{1}{\tau_D}=\left(\frac{4\hbar^3k_f^5}{\pi^3a(\mu^*)^2n_1k_BT}\right)\sum_{\Delta m}\int_0^\infty\int_0^\infty\mathrm{d}Q\,\mathrm{d}\Omega\;Q^2|e\phi_{\Delta m}(Q)|^2$$
$$\times\frac{\mathrm{Im}\ \chi_{0,0;a}(q,\Delta m,\omega)\,\mathrm{Im}\ \chi_{0,0;b}(q,\Delta m,\omega)}{\sinh^2(\beta\Omega)} \tag{16}$$

where $Q=q/(2k_f^{(a)})$, $\Omega=\hbar\omega/(4E_f^{(a)})$, $\beta=2E_f^{(a)}/(k_BT)$. In this paper, frequency ω and wave vector q are reduced by $4E_f^{(a)}/\hbar$ and $2k_f^{(a)}$ in which $E_f^{(a)}$ and $k_f^{(a)}$ are the Fermi energy and Fermi wave vector of the inner CDW respectively. The remaining task is to carry out the integrations in equation (16) for several different sets of circumstances.

4. The polarizability of a CDW

The imaginary part of the polarizability of a CDW with radius r_0 at absolute zero temperature is [6, 7]

$$\mathrm{Im}\ \chi_{0,0;r_0}(Q,\Delta m,\Omega)=\sum_m\mathrm{Im}\ \chi^{(m)}_{0,a;r_0}(Q,\Delta m,\Omega) \tag{17}$$

where the angular quantum number m and Δm are equal to 0, ± 1, ± 2, ... $\pm m^0$, and

$$m^0 = \lceil k_f^{(r_0)} r_0 \rceil \tag{18}$$

which denotes the integral part of $k_f^{(r_0)} r_0$, and

$$\mathrm{Im}\chi^{(m)}_{0,0;r_0}(Q, \Delta m, \Omega) = \left(-\frac{\mu^*}{2\hbar^2 k_f^{(a)} Q}\right)\Big\{H[k_z^{(r_0)}(m) - |k_f^{(a)}(N(m) - \Omega/Q)|] - H[k_z^{(r_0)}(m) - |k_f^{(a)}(N(m) + \Omega/Q)|]\Big\} \tag{19}$$

in which $H(x)$ is the Heaviside unit step function. The effective wave vector

$$k_z^{(r_0)}(m) = [(k_f^{(r_0)})^2 - m^2/r_0^2]^{1/2} \tag{20}$$

and

$$N(m) = Q + \frac{m\ \Delta m}{2(k_f^{(a)} r_0)^2 Q} + \frac{(\Delta m)^2}{(2k_f^{(a)} r_0)^2 Q}. \tag{21}$$

The Fermi wave vector $k_f^{(r_0)}$ is determined by

$$n_0 \pi^2 r_0^2 = k_f^{(r_0)} r_0 + 2[(k_f^{(r_0)} r_0)^2 - 1]^{1/2} + \cdots + 2[(k_f^{(r_0)} r_0)^2 - \lceil k_f^{(r_0)} r_0 \rceil^2]^{1/2} \tag{22}$$

where n_0 is the electron area density. Strictly speaking we should use here the finite-temperature expression for Im $\chi_{0,0;r_0}$. This, however, owing to the step-like structure of the energy dependence of Fermi equilibrium distribution function f^0, would only affect the momentum relaxation rate to higher order in T/T_f. We may therefore use the zero-temperature expression, since we are concerned with the variations not on the scale of the Fermi temperature, but on a much smaller temperature scale set by the distance d between the two CDWs. Obviously the maximum angular quantum number m^0 is related to radius r_0. There is a critical radius r_c which is determined by $1/(\pi n_0^{1/2})$. For example, in the case where $n_0 = 1.5 \times 10^{11}$ cm^{-2}, $r_c \simeq 82.187$ Å. When $r_0 < r_c$, $m^0 = 0$, the electrons in the CDW reduce to a one-dimensional electron gas [8, 9].

In terms of the Green's function in cylindrical coordinates

$$G_{\Delta m}(r, r') = \begin{cases} K_{\Delta m}(qr) I_{\Delta m}(qr') & \text{if } r' \leqslant r \\ I_{\Delta m}(qr) K_{\Delta m}(qr') & \text{if } r' \geqslant r. \end{cases} \tag{23}$$

The Fourier transform of the effective interaction can be obtained by solving Poisson's equation for the potential [5]

$$e\phi_{\Delta m}(q) = \left(\frac{4\pi e^2}{\kappa}\right) \frac{I_{\Delta m}(qa) K_{\Delta m}(qb)}{\Delta} \tag{24}$$

where $K_m(x)$ and $I_m(x)$ are the mth-order modified Bessel functions and

$$\Delta = [1 + 2q_{TF}^{(a)} a K_{\Delta m}(qa) I_{\Delta m}(qa)][1 + 2q_{TF}^{(b)} b K_{\Delta m}(qb) I_{\Delta m}(qb)] - 4q_{TF}^{(a)} q_{TF}^{(b)} ab [I_{\Delta m}(qa) K_{\Delta m}(qb)]^2 \tag{25}$$

where κ is the dielectric constant and the Fermi–Thomas screening wave vector is determined by

$$q_{TF}^{(r_0)} = \frac{2\pi e^2}{\kappa} \frac{\mathrm{d}n_0}{\mathrm{d}E_f^{(r_0)}}$$

$$= \frac{2e^2\mu^*}{\kappa\pi\hbar^2(k_f^{(r_0)}r_0)}\left\{1+\frac{2k_f^{(r_0)}r_0}{[(k_f^{(r_0)}r_0)^2-1^2]^{1/2}}+\cdots+\frac{2k_f^{(r_0)}r_0}{[(k_f^{(r_0)}r_0)^2-(m^0)^2]^{1/2}}\right\}. \tag{26}$$

To get this equation, we have used the expression for n_0 given by equation (22).

5. Results and discussion

We define

$$\Gamma(Q,\Omega) = \sum_{\Delta m} \operatorname{Im}\chi_{0,0;a}(Q,\Delta m,\Omega)\operatorname{Im}\chi_{0,0;b}(Q,\Delta m,\Omega)$$
$$= \sum_{\Delta m}\sum_{m}\sum_{m'} \operatorname{Im}\chi^{(m)}_{0,0;a}(Q,\Delta m,\Omega)\operatorname{Im}\chi^{(m')}_{0,0;b}(Q,\Delta m,\Omega). \tag{27}$$

By using the step-like function behaviour of the Heaviside unit step function, it can be proved from equation (19) that

$$\operatorname{Im}\chi^{(m)}_{0,0;r_0} = \begin{cases} -\left(\dfrac{\mu^*}{2\hbar^2k_f^{(a)}Q}\right) & \text{if } \Omega_m^{r_0^-} < \Omega < \Omega_m^{r_0^+} \\ 0 & \text{otherwise} \end{cases} \tag{28}$$

where

$$\Omega_m^{r_0^\pm} = \left|\left[Q^2+(M_{r_0}^m)^2\right] \pm Q\gamma_{r_0}^m\right| \tag{29}$$

and

$$\gamma_{r_0}^m = k_z^{(r_0)}(m)/k_f^{(a)} \tag{30}$$

in which the effective wave vector, $k_z^{(r_0)}(m)$, is defined by equation (20) and

$$M_{r_0}^m = \frac{\sqrt{(m+\Delta m)^2-m^2}}{2k_f^{(a)}r_0}. \tag{31}$$

Then $\Gamma(Q,\Omega)$ is an Ω-independent constant in the region of $\Omega^- < \Omega < \Omega^+$ and is zero otherwise. The integration over Ω in equation (16) may be carried out analytically to yield

$$\frac{1}{\tau_D} = \left(\frac{\mu^*k_f^{(a)}}{\pi^3\hbar^3an_1}\right)\sum_{\Delta m}\sum_{m}\sum_{m'}\int_0^\infty \mathrm{d}Q\ |e\phi_0(Q)|^2[\operatorname{cotanh}(\beta\Omega^-)-\operatorname{cotanh}(\beta\Omega^+)] \tag{32}$$

where the $\Omega^\pm$ are defined by

$$\Omega^+ = \begin{cases} \Omega_m^{a^+} & \text{if } \Omega_m^{a^+} < \Omega_{m'}^{b^+} \\ \Omega_{m'}^{b^+} & \text{if } \Omega_m^{a^+} > \Omega_{m'}^{b^+} \end{cases} \tag{33}$$

and

$$\Omega^- = \begin{cases} \Omega_m^{a^-} & \text{if } \Omega_m^{a^-} > \Omega_{m'}^{b^-} \\ \Omega_{m'}^{b^-} & \text{if } \Omega_m^{a^-} < \Omega_{m'}^{b^-}. \end{cases} \tag{34}$$

If the radii of inner and outer CDWs of a coupled CDW system, a and b, satisfy $a < r_c < b$, it becomes a coupled 2D−1D CDW system for the reasons discussed above. Such systems are expected to have characteristics of Coulomb drag which are different from those exhibited by both the coupled 1D−1D system and the 2D−2D system. Because

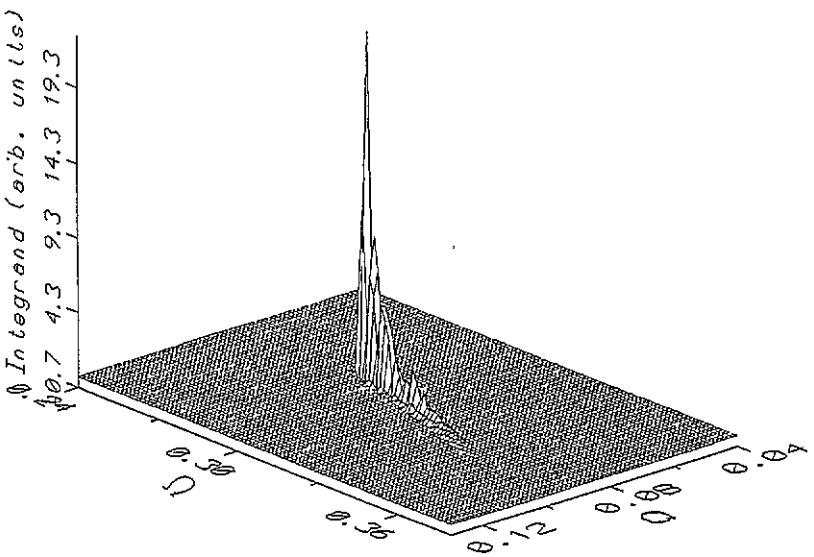

Figure 2. The dependence on Q and Ω of the integrand in equation (15) for $T = 13$ K.

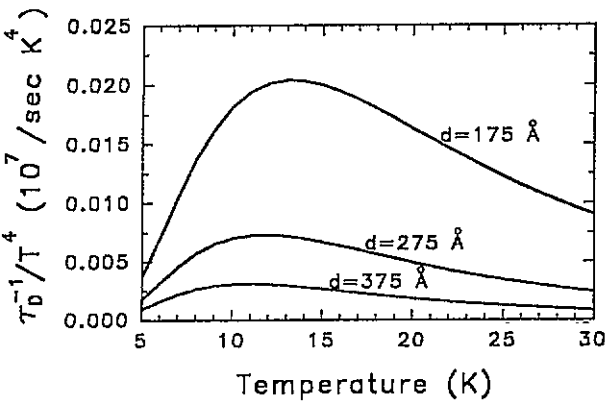

Figure 3. A plot of the theoretical values of $1/(\tau_D T^4)$ as functions of temperature, for $d = 175$, 275 and 375 Å.

$a < r_c$, $m^0 = 0$, so both m and Δm are equal to zero. The summation over Δm in equation (27) can be cancelled while we set $\Delta m = 0$ in it. And it may be proved that when $\Delta m = 0$, for both 1D and 2D CDW [9],

$$\text{Im } \chi^{(m)}_{0,0;r_0} = \begin{cases} -\left(\dfrac{\mu^*}{2\hbar^2 k_f^{(a)} Q}\right) & \text{if } \Omega_m^{r_0^-} < \Omega < \Omega_m^{r_0^+} \\ 0 & \text{otherwise} \end{cases} \tag{35}$$

where

$$\Omega_m^{r_0^\pm} = |Q^2 \pm Q\gamma_{r_0}^m| \tag{36}$$

in which $\gamma_{r_0}^m$ is defined by equation (30). In particular, for the inner CDW $m = 0$ since $a < r_c$, and thus

$$\Omega_0^{a\pm} = |Q^2 \pm Q|. \tag{37}$$

By using equations (35)–(37), it may be proved that

$$\Gamma(Q,\Omega) = \begin{cases} \sum_m \left(\dfrac{\mu^*}{2\hbar^2 k_f^{(a)} Q}\right)^2 & \text{if } \Omega_{min} < \Omega < \Omega_{max} \\ 0 & \text{otherwise} \end{cases} \tag{38}$$

where

$$\Omega_{max} = \Omega_m^{b+} = |Q^2 + Q\gamma_b^m| \tag{39}$$

and

$$\Omega_{min} = \begin{cases} Q - Q^2 & \text{if } Q < (1+\gamma_b^m)2 \\ Q(Q-\gamma_b^m) & \text{if } Q > (1+\gamma_b^m)/2. \end{cases} \tag{40}$$

Attention must be paid to the fact that when $Q = Q_{min} = (1-\gamma_b^m)/2$, $\Omega_{min} = \Omega_{max}$. So we have $\Gamma(Q,\Omega) = 0$ when $Q < Q_{min}$. Obviously for coupled 2D–1D CDWs, $\Gamma(Q,\Omega)$ is a Ω-independent constant in the region $\Omega_{min} < \Omega < \Omega_{max}$ and zero otherwise. Therefore we can also complete the integration over Ω in equation (16) analytically, and get the expression for the momentum relaxation rate:

$$\frac{1}{\tau_D} = \sum_m \left(\frac{1}{\tau_D^{(m)}}\right) = \left(\frac{\mu^* k_f^{(a)}}{\pi^3\hbar^3 a n_1}\right) \sum_m \int_0^\infty \mathrm{d}Q\ |e\phi_0(Q)|^2 [\mathrm{cotanh}(\beta\Omega_{min}) - \mathrm{cotanh}(\beta\Omega_{max})]. \tag{41}$$

The parameters used in the numerical calculation are the electron area densities in the two CDWs, $n_1 = n_2 = 1.5 \times 10^{11}$ cm^{-2}. The effective mass $\mu^* = 0.067m_0$ and the dielectric constant $\kappa = 13$.

5.1. The momentum relaxation rate of the coupled 2D–1D CDWs

First of all, we study the momentum relaxation rate of the barrier-coupled 2D–1D CDWs of which the radii of inner and outer CDWs satisfy $a < r_c < b$ [11]. We take the radius of the inner CDW to be $a = 80$ Å. Then the Coulomb drag behaviour of barrier-coupled 2D–1D CDWs can be yielded by carrying out the integration over Q and summation over m in equation (41).

We show in figure 2 the dependence for Q and Ω of the integrand in equation (16). Note that the integrand vanishes in the region of reduced wave vector $Q < Q_{min} = (1-\gamma_b^m)/2$.

Figure 3 shows the numerical results for $1/(\tau_D T^4)$ as functions of temperature in the region $T = 5$–30 K, calculated from equation (41) for three different values of the separation distances, $d = 175$, 275 and 375 Å. The maximum values of $1/(\tau_D T^4)$ occur at around $T = 12$ K which is about nine times less than T_f.

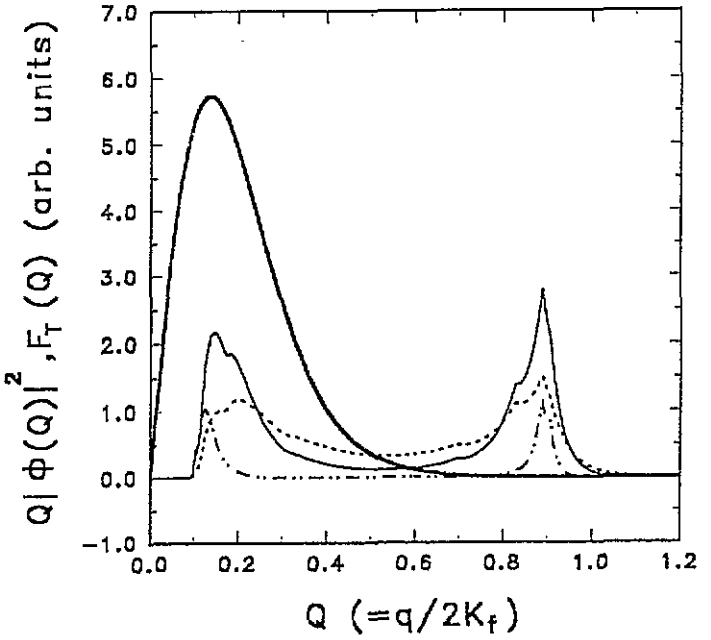

Figure 4. The interaction term $Q|e\phi_0(Q)|^2$ (the thick full curve) and the phase-space term $F_T(Q)$ for temperatures $T = 12$ K (the thin full curve), $T = 5$ K (the chain curve) and $T = 20$ K (the short-dashed curve).

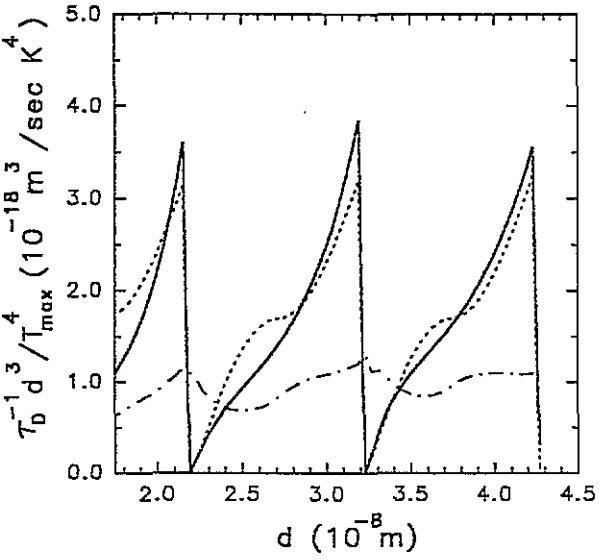

Figure 5. A plot of $d^3/[\tau_D(T_{max})^4]$ as a function of distance d.

To gain a better understanding of the physics underlying the nonmonotonic temperature dependence of $1/(\tau_D T^4)$, following the method of Jauho and Smith [5], we rewrite equation (41) as

$$1/(\tau_D T^4) = \int_0^\infty \mathrm{d}Q\ Q|e\phi_0(Q)|^2 F_T(Q) \tag{42}$$

where $F_T(Q)$ is the result of the Ω integration in equation (16) which has been completed analytically. The two factors in the Q-integral of equation (42) have different physical origins: the $Q|\phi_0(Q)|^2$-term describes the Q-dependence of the interaction, while the $F_T(Q)$-section is related to the phase space corresponding to the momentum transfer $\hbar Q$. These two terms are plotted as functions of Q in the case where $d = 275$ Å in figure 4. The function $F_T(Q)$ is strongly temperature dependent; the maximum peak height changes as the temperature changes. At a certain temperature ($T = 12$ K in the present example), the peaks of the two terms coincide and reach maximum overlap, resulting in the maximum value of $1/(\tau_D T^4)$.

In figure 5, the dependence of $d^3/[\tau_D(T_{max})^4]$ on the separation distance d is plotted. The full curve shows the numerical result calculated from equation (41). The short-dashed curve is given by a nearly periodic analytical function which is used to fit the numerical result:

$$\frac{d^3}{\tau_D(T_{max})^4} = C\left[1 - \eta + \eta\left|\sin\left(\pi\frac{d-d_0}{d_T}\right)\right|\right] \tag{43}$$

where $C = 1.70 \times 10^{-18}$ m^3 s^{-1} K^{-4}, $d_0 = 117$ Å, and $\eta = (-1)^{[(d-d_0)/(d_T/2)]}$, in which $[x]$ means the integral part of x, and the period

$$d_T = r_0^{(n+1)} - r_0^{(n)} \tag{44}$$

where the $r_0^{(n)}$ are a series of special radii of a CDW which satisfy the condition

$$k_f^{(r_0^{(n)})} r_0^{(n)} = n \tag{45}$$

in which n is an integer.

The chain curve is used to denote the numerical value of $d^3/[\tau_D(T_{max})^4]$ divided by its analytical value given by equation (43). Its gentle variation versus distance d proves that the numerical value is well fitted by the analytical one.

Figure 6, upper panel, shows the plot of T_{max} as function of d, and figure 6, lower panel, shows the plot of the logarithm of T_{max} as a function of the logarithm of d (Å). The short-dashed curves in figure 6 show the results calculated from an analytical function used to simulate roughly the numerical results:

$$T_{max} = 0.49\pi^5(q_{TF}^{(a)}d)^{-0.14}\left(1 + \frac{3.6\pi^2\cos^2[2\sqrt{\pi}(d/d_T + 0.124)]}{d}\right) \tag{46}$$

where d_T is defined by equation (44). The chain line in figure 6, lower panel, is the best-fit line obtained using a linear fitting equation of which the slope is $\alpha = -0.14$.

The physical origin of the oscillatory behaviour of the momentum relaxation rate as shown in figure 5 is the oscillation of the Fourier transform of the effective interaction $\phi_{\Delta m}(q)$. We can see from equation (24) that the strength of the screening effect in a coupled CDW system is determined by Δ defined in equation (25). When the radius of the inner CDW, a, is fixed, Δ is an oscillatory function of b (or $d = b - a$) as the result of the oscillation of a dimensionless screening wave vector in the Fermi–Thomas approximation, $q_{TF}^{(b)}b$, with respect to b (or d) with the oscillation period d_T. Since according to equations (26) and (45), in the range of a period, $q_{TF}^{(b)}b$ tends to infinity when $b - r_0^{(n)}$ tends to 0^+ (i.e., $k_f^{(b)}b - n$ tends to 0^+), then it attenuates quickly as the value of $b - r_0^{(n)}$ increases and $q_{TF}^{(b)}b$ reaches its minimum value when $b - r_0^{(n+1)}$ tends to 0^- (i.e., $k_f^{(b)}b - (n+1)$ tends to 0^-). As a result, $\phi_{\Delta m}(q)$ and the momentum relaxation rate show oscillatory behaviour. It can be calculated from equations (22) and (45) that $r_0^{(n)} = 82.187$, 192.116, 297.792, 402.340 and 506.390 Å when $n = 1$, 2, 3, 4 and 5, so $b = r_0^{(n)}$ when the separation distance d is

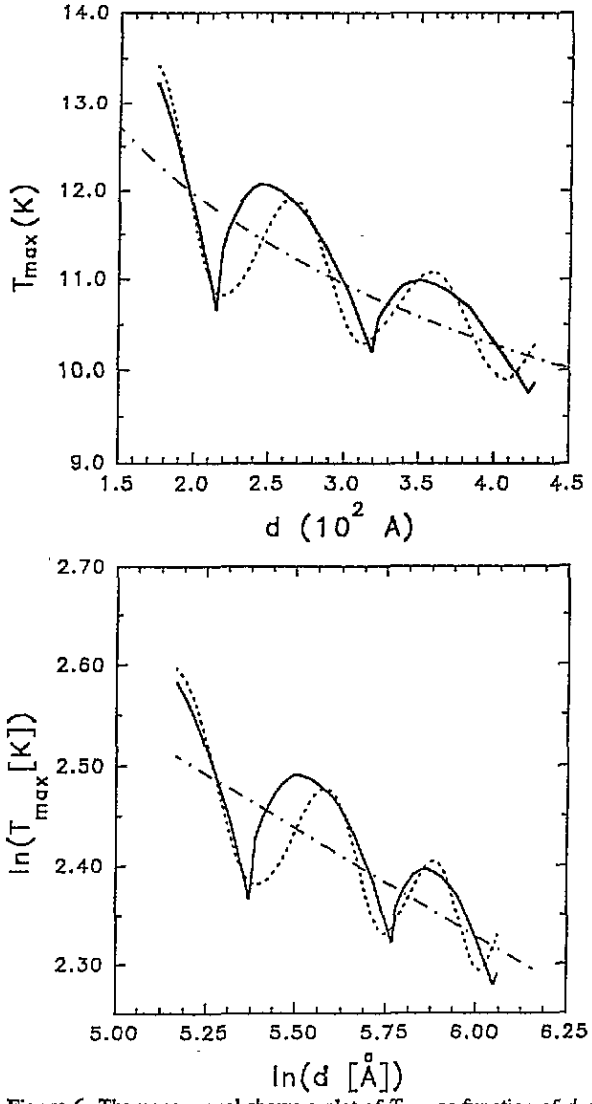

Figure 6. The upper panel shows a plot of T_{max} as function of d, while the lower panel shows the dependence of the logarithm of T_{max} as a function of the logarithm of d (Å). d is the distance between two coaxial CDWs.

equal to 2.187, 112.116, 217.792, 322.340 and 426.390 Å. We can see from figure 5 that when d increases and passes across these values from left to right, the momentum relaxation rate jumps rapidly from its peak values to zero, then increases monotonically again as d increases until the next jumping point is reached.

5.2. The momentum relaxation rate of the barrier-coupled 2D–2D CDWs and the transition behaviour on going from coupled 2D–1D to coupled 2D–2D CDWs

Finally, we discuss the Coulomb drag resistivity between a 2D CDW and a 2D CDW, and the transition behaviour of Coulomb drag on going from coupled 2D–1D CDWs to coupled 2D–2D CDWs. We consider a coupled CDW system of which the radii of the inner and

outer CDWs, a and b, are both greater than r_c. Such of systems are expected to have characteristics of Coulomb drag similar to those of barrier-coupled 2D–2D planes. In the first example, we take $a = 150$ Å and $b = 350$, 375 and 425 Å while maintaining the values of all the other parameters. This corresponds to $m^0 = 2$, $m^{0'} = 3$, 3 and 4 and $\Delta m = 0$, ± 1 ± 2 in equations (27) and (32) from which τ_D^{-1} can be calculated as a functions of T and d.

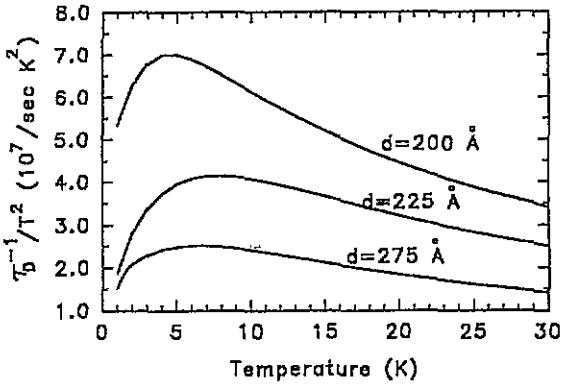

Figure 7. A plot of $1/(\tau_D T^2)$ as a function of temperature in the range from $T = 0$ to 30 K for different values of the distance, $d = 200$, 225 and 275 Å, when $a = 150$ Å.

In figure 7 we have plotted $1/(\tau_D T^2)$ as a function of temperature in the range from $T = 0$ to 30 K for different values of the distance, $d = 200$, 225 and 275 Å. The maximum values of $1/(\tau_D T^2)$ occur at around $T_{max} \simeq 6$ K. This behaviour is in accord with the characteristics of momentum relaxation rates in barrier-coupled 2D–2D planes as shown in figure 3 of [5] and figure 3 of [10] where T_{max} is roughly equal to 10 K and 2 K respectively. In the case where $d = 225$ Å, for coupled 2D–2D CDWs, the value of $1/(\tau_D T_{max}^2) \simeq 4.2 \times 10^7$ s^{-1} K^{-2}, which is about 20 times bigger than that of the experimental data of the coupled 2D–2D plane given in [10]. We can see from these results that when we increase the radius of the inner CDW of coupled CDWs from $a = 80$ Å ($<r_c$) to $a = 150$ Å ($>r_c$), the characteristic behaviour of the momentum relaxation rate as a function of temperature transforms from 2D–1D behaviour to typical 2D–2D behaviour which is maintained until rather bigger values of a are reached. For example when $a = 600$ Å, $d = 225$ Å and $d = 275$ Å, the curves of $1/(\tau_D T^2)$ versus temperature T have maximum values at around $T_{max} = 2$ K.

Figure 8 is a plot of $d^{2.4}/[\tau_D (T_{max})^2]$ as a function of distance d in the case where $a = 600$ Å. Similarly to the results from figure 5 for coupled 2D–1D CDWs, equation (43) with $C = 6.6 \times 10^{-12}$ m$^{2.4}$ s^{-1} K^{-2}, $d_0 = 114$ Å and d_T determined by equation (44) can be used to fit roughly the numerical results plotted in figure 8; i.e., for coupled 2D–2D CDWs, τ_D^{-1}/T_{max}^2 is roughly proportional to $d^{-2.4}$ times a nearly periodic function of d with period d_T. This is quite different from the $d^{-2.4}$-dependence of τ_D^{-1}/T_{max}^2 in coupled 2D–2D planes, because, according to the results of [5], τ_D^{-1} and T_{max} are proportional roughly to d^{-4} and $d^{-0.8}$ respectively. So τ_D^{-1}/T_{max}^2 is roughly proportional to $d^{-2.4}$. This discrepancy originates from the quantization of the circular motion round the cylindrical symmetry axis.

To study the behaviour of the Coulomb drag of coupled CDWs in the region where $a \simeq r_c$, in figure 9 we plot τ_D^{-1}/T^n as function of T for differential values of n for both $a = 110$ Å and $a = 120$ Å in the case where $d = 175$ Å. The dashed curves are used to

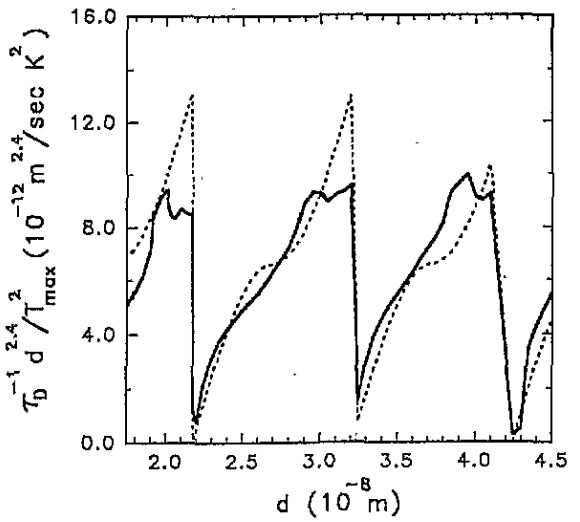

Figure 8. A plot of $d^3/[\tau_D(T_{max})^2]$ as a function of distance d. The full curve shows the numerical result calculated from equation (32). The short-dashed curve is given by a nearly periodic analytical function, equation (43), which is used to fit the numerical result.

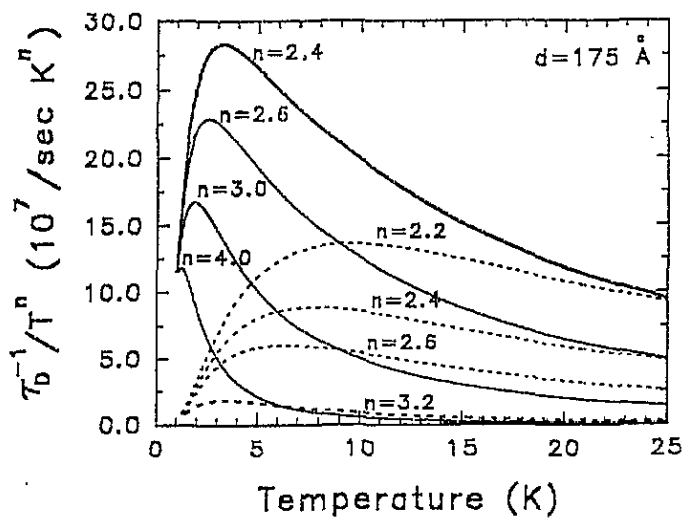

Figure 9. A plot of $1/(\tau_D T^n)$ as a function of T for different values of n for $a = 110$ Å and $a = 120$ Å in the case where $d = 175$ Å.

denote the results of taking $a = 110$ Å and the full curves are those for $a = 120$ Å. It is clear that over the whole ranges of temperatures, when $a = 110$ and 120 Å the momentum relaxation rates, τ_D^{-1}, are roughly proportional to $T^{3.2}$ and $T^{2.4}$ respectively, while when $a \gtrsim 150$ Å the rate is proportional to T^2.

6. Conclusion

In this paper we have discussed the rate of momentum relaxation between two electron gases confined in two cylindrical delta quantum wells with a common cylindrical symmetry

axis which are coupled via screened Coulomb interaction. The results are that for coupled 2D−1D CDWs the momentum relaxation rate, τ_D^{-1}, is approximately proportional to T^4, while for coupled 2D−2D CDWs it is proportional to T^2, which is in accord with the characteristic behaviour of the momentum relaxation rate in coupled 2D−2D planes. In the transition region from coupled 2D−1D to 2D−2D CDWs, τ_D^{-1} is proportional to T^n with n reducing from 4 to 2 gradually. In addition, quite different from the $d^{-2.4}$-dependence of the momentum relaxation rate divided by T_{max}^2 in coupled 2D−2D planes, due to the quantization of the circular motion round the cylindrical symmetry axis, for coupled 2D−1D CDWs, the momentum relaxation rate divided by T_{max}^4 is approximately proportional to d^{-3} times a nearly periodic function of d with period d_T—while for coupled 2D−2D CDWs, the momentum relaxation rate divided by T_{max}^2 is approximately proportional to $d^{-2.4}$ times a nearly periodic function of d with period d_T.

The calculation of the Coulomb drag resistivity under a magnetic field along the cylindrical symmetry axis (the z-direction) in coupled cylindrical delta quantum wells is under way.

Acknowledgment

This work was supported by the National Science Foundation of China.

References

[1] Hodges C, Smith H and Wilkins J W 1971 *Phys. Rev.* B 4 302
[2] Laikhtman B and Solomon P M 1990 *Phys. Rev.* B **41** 9921
[3] Solomon P M and Laikhtman B 1991 *Superlatt. Microstruct.* **10** 89
[4] Maslov D I 1992 *Phys. Rev.* B 45 1911
[5] Jauho A and Smith H 1993 *Phys. Rev.* B 47 4420
[6] Chen Hao, Zhu Yun and Zhou Shixun 1987 *Phys. Rev.* B 36 8189
[7] Zhu Yun, Huang Feng-yi, Xiong Xiao-ming and Zhou Shixun 1988 *Phys. Rev.* B 37 8992
[8] Qin G and Shen R 1994 *Solid State Commun.* 89 301
[9] Friesen W I and Bergersen B 1980 *J. Phys. C: Solid State Phys.* 13 6627
[10] Gramila T J, Eisenstein J P, MacDonald A H, Pfeiffer L N and West K W 1991 *Phys. Rev. Lett.* 66 1216
[11] Qin G 1995 *Solid State Commun.* 95 701